World Journal of Advanced Research and Reviews
eISSN: 2581-9615 CODEN (USA): WJARAI
Cross Ref DOI: 10.30574/wjarr
Journal homepage: https://wjarr.com/

(RESEARCH ARTICLE)

Check for updates

Batch adsorption of safranin dye from aqueous solution using activated groundnut pods (AGP)

James Akande Asamu [1,*], Omotola Fayomi Michael [2] and Kehinde Makinde Olaoluwa [3]

[1] *Department of Chemistry and Biochemistry, Caleb University, Imota Lagos, Nigeria.*
[2] *Department of Chemistry, Federal University of Agriculture, Makurdi, Nigeria.*
[3] *Department of Chemistry, Lagos State University, Ojo, Nigeria.*

World Journal of Advanced Research and Reviews, 2022, 16(02), 403–423

Publication history: Received on 30 September 2022; revised on 06 November 2022; accepted on 09 November 2022

Article DOI: https://doi.org/10.30574/wjarr.2022.16.2.1158

Abstract

This work aimed on the adsorption of safranin dye from wastewater using activated groundnut pods (AGP). The raw pods were collected, crushed into particle size of about 400 - 550 µm and modified *in-situ* with $ZnCl_2$ to prepare AGP which was characterized using analytical technique; Fourier Transform Infra-Red (FTIR), Energy Dispersive X-ray (EDX) spectroscopy, Thermo gravimetric analyser (TGA) and Scanning Electron Microscopy (SEM). The absorbance of the dye solution was monitored at 530 nm with UV-Visible spectrophotometer. FTIR analysis showed the vibration frequency for C–H, O–H, C=O and C–O stretches at 2900, 3420, 1730, and 1100 cm^{-1} respectively. SEM results revealed the AGP has a porous surface with heterogeneous pores which became compact after dye adsorption. EDX confirmed the presence of C, O, Zn and Cl in the adsorbent. The suitability of the pseudo-first, pseudo second and Elovich kinetic models for the sorption of safranin onto AGP was examined. The equilibrium data were subjected to Langmuir, Freundlich, Tempkin and Dubinin-Radushkevich isotherm models. Adsorption factors were optimized by Box-Behnken design using response surface methodology (RSM). The pseudo-second order kinetic model provided the best correlation and was found to be more statistically significant. Langmuir model was found to fit well based on the high values of the coefficient of regression R^2 and low % standard error values. The monolayer adsorption capacity Q_{max} was found to be 45.45 mgg^{-1}. Thermodynamic adsorption processes showed the spontaneous, endothermic and randomness of the systems with free energy change less than zero, enthalpy change (ΔH) of 66.43 $kJmol^{-1}$and entropy change (ΔS) of 145.37 $Jmol^{-1}K^{-1}$. Response Surface Methodology (RSM) showed that 0.55 g was the optimum dosage with 92.50 % removal of safranin dye concentration of 200 mgL^{-1} at pH 10.

Keywords: Kinetic; Adsorption; Safranin; Activated groundnut pod; Isotherm; Response surface

1. Introduction

Some toxic dyes caused severe damage to human organs such as kidney, reproductive system, liver, brain and central nervous system. When inhaled, there are possible health symptoms such as difficulties in breathing, vomiting, dermatitis, diarrhea and cancer. They are highly stable compounds to light, chemical, biological and other exposures[1]. Dyes are basically natural or synthetic organic compounds that can connect themselves to surfaces or fabrics to produce bright and lasting colour [2]. Synthetic dyes are one of the major water pollutants mostly released from various industrial processes such as dyestuff manufacturing, dyeing, printing, textile finishing, etc. Annually, 12 % of the synthetic dyes are discharged into aquatic body from anthropogenic activities. The textile industries account for two thirds of the world's annual production estimated to be 7 x 10^5 tonnes [3]. Pollution from this source are the major concern for the developing countries because of various factors such as visibility of dyes even in low concentrations; adverse effect on the photosynthetic activities of the aquatic life among others. It is necessary to effectively treat

* Corresponding author: Akande, James Asamu
Department of Chemistry and Biochemistry, Caleb University, Imota Lagos, Nigeria.

effluents containing dyes due to the environmental and toxicology threats posed to human and aquatics animals. Colour removal is one of the daunting tasks faced by industries, while the development of cost effective and environmentally safe method in dyes adsorption is challenging to researchers. Many processes such as liquid–liquid extraction[4], ozonation, adsorption [5] etc, have been adopted to dyes removal in wastewater. However; some of these techniques are inefficient and expensive to treat wastewater containing dyes. Adsorption technique has been found to be a superior separation and purification method because of its easy-nature, low cost, high selectivity and high removal efficiency.

Most countries of the world are agrarians with abundant cellulosic by-products from the production of crops such as groundnuts, millet, soybean rice etc. The natural fiber comes from stalks, leaves and seeds, such as kenaf, sisal, flax, sorghum, wheat and rice [6]. Natural fiber have been found to be advantageous over the synthetic ones in terms of biodegradability, flammability and non-toxicity [7].Cellulose, a biopolymer is considered a promising natural source that has been extensively explored by researchers for adsorption. Surface modification of cellulose improves its potential in adsorption process, hence, needs to modify the groundnut pods in this work. Also thermal and mechanical resistance may also increase its pollutant adsorption capacity in aqueous and non-aqueous solutions [8].Therefore, this work aimed at investigating the adsorption of safranin dye from the aqueous solutions using activated groundnut pods (AGP) as adsorbent. The kinetic, isotherm and thermodynamic parameters of the adsorption were considered in a batch process. Added was the optimization of the factors affecting the adsorption process.

2. Material and methods

2.1. Materials

Safranin O (Fig. 1) is a chloride salt of 3,7-diamino-5-phenylphenazin-5-ium and zinc chloride ($ZnCl_2$) were obtained from Merck laboratory, India. Hydrochloric acid (HCl), Urea (CH_4N_2O) and Sodium hydroxide (NaOH) were procured from BDH, London. Other reagents used were of analytical grade.

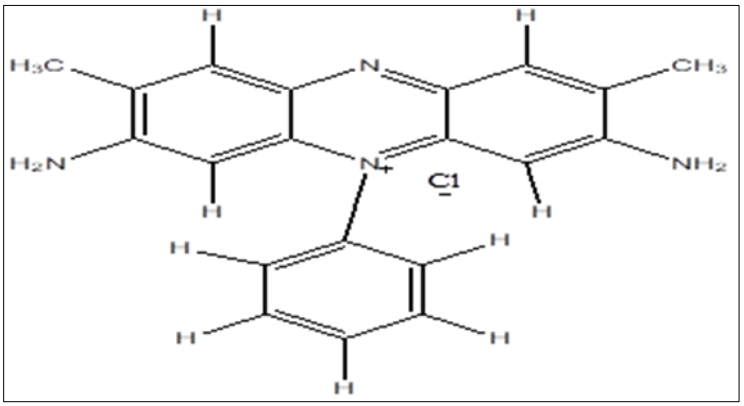

Figure 1 Structure of Safranin dye

2.2. Characterization

Scanning electron microscopy (SEM; Hitachi S4800) equipped with EDAX was used to determine the surface morphology of the adsorbent before and after adsorption, while the EDAX monitored the elemental component of the adsorbent. Organic functionalities were determined by Fourier transform infrared (FTIR) spectroscopy and recorded from 400 to 4000 cm-1 in TENSOR 27 Spectrophotometer (Bruker, Germany) using KBr pellet technique**.**

2.3. Synthesis of activated groundnut pods (AGP)

Groundnut pods were packed from a nearby market, washed with tap water and rinsed with distilled water to remove dust and impurities. The pods were air-dried then oven dried at 50 °C to constant mass. The dried pods were pulverized, sieved to obtain particle sizes less than 600µm and preserved in an air-tight polythene bag to prevent from moisture and made ready for the analysis.

The sieved pods (10.5 g) were suspended in 30 ml of 0.2M $ZnCl_2$, 10 ml of 2M urea solution was added as a stabilizer and stirred continuously for 1hr on a magnetic stirrer. The suspension was centrifuged, washed thoroughly with distilled water till a neutral pH attained. It was then dried in a vacuum oven at 343K and kept in an air tight container.

2.3.1. Preparation of adsorbate

Safranin dye (1.0 g) was dissolved in 1litre of distilled water to give a concentration of 1000 mgl^{-1}. Experimental solutions were prepared form the stock solution through appropriate dilution.

$$C_1V_1 = C_2V_2 \text{…….} (1)$$

2.3.2. Determination of Thermodynamic Parameters

The influence of temperature on the adsorption of safranin ions studied on AGP was studied at 30 –70 °C, other parameters being kept constant. The 50 mL of 50 mg/L of Safranin dye was prepared and had its pH adjusted to neutral with 0.01M NaOH and 0.01M HCl. Two separate 25 mL of the solution had 0.1g of adsorbent to one of them and the other served as the blank. The two solutions were agitated in a thermostated shaker at150 rpm for 4 hours. The absorbance of the solutions were monitored on a uv- visible spectrophotometer [22].

2.3.3. Determination of solution pH

The effect of solution pH on safranin dye removal from aqueous solution was studied under identical conditions. The concentration of the dye (100 mgL-1) was prepared in ten 50 mL Erlenmeyer flasks followed by pH adjustment (2 – 12), 0.25 g of the adsorbent was added to each of the dye solutions. Along with the blank solution, all the flasks were placed in a thermostated shaker at 30 oC and 150 rpm for 4 hours to reach equilibrium. The absorbance readings were taken on uv- visible spectrophotometer.

2.4. Adsorbent dosage experiment

To determine the effect of adsorbent dosage, 100 mgL^{-1}dye solution was prepared, followed by pH adjustment to 7 with 0.01M HCl and 0.01M NaOH. 25 ml of dye solution was transferred into ten Erlenmeyer flasks each with 0.1 – 2.0 g adsorbent added. Along with the blank, all the flasks were placed in a thermostated shaker at 30 ^oC and 150 rpm for 4 hours. The absorbance readings were taken on uv- visible spectrophotometer at 530 nm.

2.4.1. Effect of contact time and dye concentration

Kinetic of safranin dye adsorption onto AGP was investigated in a batch experiment by adding 0.25 g of adsorbent into forty five 100 ml Erlenmeyer flasks containing 25 mL of the dye solution of the concentration range between 50 – 250 mgl^{-1}. The pH of the dye was adjusted by adding 0.01 M HCl and 0.01 M NaOH to get the desired neutral pH. The flasks were then transferred into a thermostated shaker at 30 ± 1 ^oC and 150 rpm, each of the flasks was removed at pre-set time interval 5 to 240 minutes. The samples were centrifuged and the concentrations of safranin dye remaining in the supernatants were determined with the uv-spectrophotometer at 530 nm wavelength. The procedure was duplicated with three absorbance reading to the average. The amount of safranin dye adsorbed onto the adsorbent at the given time was calculated by the equation:

$$Q_t = \frac{(C_o - C_t) \times V}{M} \text{……} (2)$$

Where Q_t is the quantity adsorbed at time‘t’ in mgg^{-1}, C_0 and C_t are the initial and final concentrations in mgL^{-1}, M is the mass of adsorbent in g, V is the volume of dye solution in litres. The adsorption kinetics were subjected to pseudo first order, pseudo second order and Elovich kinetic model in conjunction with Sum of Square Error (SSE), HYBRID fractional error function and root-mean-square error (RMSE). The error functions defined the best fitting relationships that quantify the distribution of adsorbate and also in the verification of the consistency of adsorption models and the theoretical assumptions of adsorption models. The nonlinear regression usually involved the minimization of error distribution between the experimental and calculated data based on their convergence criteria. The sum of square errors is said to be the most widely used error function and was calculated by the equation:

$$\%SSE = \frac{100}{N}\sqrt{\frac{(Q_{Exp} - Q_{Cal})^2}{Q_{Exp}}} \text{……} (3)$$

Where;
N is the number of data points.

Q_{Cal} is the theoretical concentration of adsorbate on the adsorbent,

Q_{Exp} is the experimentally measured adsorbed solid phase concentration of the adsorbate on the adsorbent.

Despite SSE as the most widely used error function, at higher end of the liquid-phase concentration ranges, the magnitude and squares of the errors tend to increase, illustrating a better fit for the isotherm parameters derivation [10]. Hybrid fractional error function was developed to improve SSE fit at low concentrations. Hereby, each SSE value was divided by the experimental solid-phase concentration with a divisor included in the system as a term for the number of degrees of freedom i.e (the number of data points minus the number of parameters within the isotherm equation) [10]. Hybrid fractional error function was developed by [11], to improve the fit of the sum square of errors SSE at low concentrations by dividing it by the measured value. This function includes the number of data points (N) minus the number of parameters (P) or isotherm equation as a divisor. The HYBRID fractional error function was calculated by the equation below:

$$\%HYBRID = \frac{100}{N-P}\sqrt{\frac{\left(Q_{Exp}-Q_{Cal}\right)^2}{Q_{Exp}}} \quad \text{.....(4)}$$

Root mean square error (RMSE) was used as a predictive capability of the model. It is known to be descriptive when the prediction capability among predictors is compared. The lower the RMSE value, the higher the accuracy, validity and good fitness of the model [12].

$$RMSE = \sqrt{\left[\frac{1}{n-2}\sum_{i=1}^{n}\left(Q_{Exp}-Q_{Cal}\right)\right]^2} \quad \text{.....(5)}$$

The coefficient of correlation R^2 represents the variance about the mean, it was used in analyzing the fitting degrees of isotherms and kinetic models with experimental data[13]. It can be given as:

$$R^2 = \frac{\sum\left(Q_{Cal}-Q_{Exp}\right)^2}{\sum\left(Q_{Cal}-Q_{Exp}\right)^2+\left(Q_{Cal}-Q_{Exp}\right)^2} \quad \text{.....(6)}$$

where Q_{Exp} and Q_{Cal} are the amount of adsorbate on the adsorbent during the experiment and obtained by kinetic and isotherm models in mgg^{-1} respectively[14]. The acceptability and best fit model for the kinetic data were based on the square of correlation coefficients R^2 and the percentage error function, i.e the difference between the Q_{cal} and Q_{exp}. The higher value of R^2 and lower error values confirmed the validity and acceptability of kinetic model[15].

2.5. Adsorption Isotherm studies

Adsorbent efficiency on adsorption of safranin dye was conducted through investigating various parameters by batch method. Adsorption isotherms are importantly described by adsorbate-adsorbent interaction with the adsorbent being critical in its optimization[16]. Thus, the correlation of equilibrium data using either a theoretical or empirical equation is essential for adsorption data interpretation and prediction. Several mathematical models can be used to describe experimental data of adsorption isotherms, the most common used isotherms are the Langmuir, Freundlich, Dubinin–Radushkevich and Temkin isotherms. They usually employed for further interpretation of the obtained adsorption data[17]. The adsorption experiments of safranin dye was subjected to the four isotherms.

The Langmuir isotherm model assumes that adsorption occurs homogeneously. The fundamental characteristic of the Langmuir isotherm model was evaluated by the separation factor (R_L) to determine the favorability of the adsorption. The nonlinear Langmuir equation used is given as:

$$Q_e = \frac{Q_{\max} b C_e}{1+bC_e} \quad \text{.....(7)}$$

Where;

Q_e and Q_{max} are quantities adsorbed at equilibrium and maximum adsorption capacity in mgg^{-1} ,

b is Langmuir constant in Lmg^{-1}.

$$Q_{max} = \frac{1}{C} \quad \text{.....(8)}$$

C and m are the intercept and slope of the nonlinear plots respectively.

$$b = \frac{1}{m/C} \quad \text{..... (9)}$$

The dimensionless R_L is an essential characteristic of the Langmuir isotherm which can be expressed as:

$$R_L = \frac{1}{1 + bC_e} \quad \text{..... (10)}$$

C_e is the equilibrium concentration in mgl^{-1}.

The Freundlich isotherm can be used in multilayer adsorption and heterogeneous surfaces with non-uniform distribution of adsorption heat. The non linear regression equation is;

$$Q_e = K_F C_e^{1/n} \quad \text{.....(11)}$$

K_F is the Freundlich constant in $g\ mg^{-1}\ min^{-1/n}$ and n is the adsorption intensity.

$$n = \frac{1}{m} \quad \text{.....(12)}$$

$$K_F = e^C \quad \text{.....13)}$$

Tempkin suggested that, due to adsorbent-adsorbate interactions, the heat of adsorption of all dyes molecules decrease with the surface coverage. In addition, it assumes that the adsorption is characterized by a uniform distribution of the binding energies up to some maximum binding energy.

$$Q_e = \frac{RT}{b_T} \ln a_T C_e \quad \text{..... (14)}$$

Where a_T and b_T are equilibrium binding constant in Lg^{-1} and Tempkin constant in $kJmol^{-1}$ respectively.

Dubinin-Radushkevich (D-R) isotherm was applied to the obtained data to deduce the heterogeneity of the apparent adsorption energy on the adsorption site of AGP. The non-linear regression equation applied can be given as:

$$Q_e = Q_s \exp(-\beta)\varepsilon^2 \quad \text{..... (15)}$$

Mean adsorption energy (E) in $KJmol^{-1}$ can be express as:

$$E = (-2\beta)^{-1/2} \quad \text{..... (16)}$$

$$\varepsilon = RT \ln\left[1 + \frac{1}{C_e}\right] \quad \text{..... (17)}$$

Q_s is the theoretical isotherm adsorption capacity in gmg^{-1},

β is the Dubinin-Radushkevich constant in mol^2kJ^{-2}.

β is the negative slope and ε is called Polanyi potential.

2.5.1. Models fitness:

In this study, the parameters of kinetic and isotherm models were determined based on the non-linear regression by using origin micromath software with the Levenberg Marquardt algorithm. To select the most suitable kinetic and isotherm model, it is necessary to evaluate their validity. Here, the validity of kinetic and isotherm models was assessed by criteria correlation coefficient, sum of squared error, the root mean square error and the hybrid fractional error function. These criteria describe the goodness of fit between the experimental and the calculated data.

2.6. Adsorption Kinetics

2.6.1. The pseudo-first order kinetic model

The model equation for the adsorption of safranin dye was proposed by Lagergren and often referred to as Lagergren equation[18], it has been used for reversible reactions with an equilibrium being established between liquid and solid phases. This model usually assumes that the dye adsorption onto a sorption site of the biomaterial and the initial surface coverage of adsorbent is zero. The nonlinear Lagergren model equation used can be expressed as:

$$Q_t = Q_e\left(1 - e^{-k_1 t}\right) \quad \text{..... (18)}$$

Where;

Q_t is the quantity adsorbed at time (t) in mgg^{-1},

Q_e is the quantity adsorbed at equilibrium in mgg^{-1}

k_1 is the pseudo-first-order rate constant in min^{-1}.

2.6.2. The Pseudo-second Order Kinetic Analysis

The kinetic rate equations can be given as:

$$\frac{dQ_t}{dt} = k_2\left(Q_e - Q_t\right)^2 \quad \text{..... (19)}$$

For the boundary conditions t=0, $Q_t = 0$, t=t and $Q_t = Q_t$

$$Q_t = \frac{Q_e^2 k_2 t}{1 + k_2 Q_e t} \quad \text{..... (20)}$$

where k_2 is the pseudo second order rate constant in $gmg^{-1}min^{-1}$ while other parameters had been explained already[19].

2.6.3. The Elovich Kinetic Analysis

The Elovich kinetic equation[20] can be expressed as:

$$\frac{dQ_t}{dt} = \alpha e^{(-\beta Q_t)} \quad \text{..... (21)}$$

Where;
α is the rate of chemisorption at zero coverage in gmg^{-1} min^{-1}
parameter β is related to the extent of surface coverage and activation energy for chemisorption in mgg^{-1}.

$$Q_t = \frac{1}{\beta}\ln(1+\alpha\beta t) \quad \text{..... (22)}$$

The parameters of the Elovich equation were obtained by fitting equation 22 in to the experimental data.

Table 1 Range of Separation Factor (RL) [21]

RL values	Adsorption process
RL = 0	Irreversible
RL> 1	Unfavourable
RL = 1	Linear
0 < RL< 1	Favourable

2.7. Optimization experiments on adsorption factors

The experimental design, regression, statistical analysis, optimization and graphical analysis were carried out with design expert software (version 6.0.8). The experiment design provides a statistical model that uses quantitative data to determine regression model equations for the optimization of operating conditions. The Box–Behnken design of response surface methodology (RSM) was employed to optimize conditions for maximum adsorption of Safranin on AGP. Statistical analysis was carried out by fitting experimental data to a general model equation.The interactive effects of the process parameters were studied using this model. Removal efficiency (RE) was calculated.

$$RE = \frac{[C_o - C_e]}{C_o} \times 100 \quad \text{.....(23)}$$

The process optimization and experimental design of the adsorption factors were designed according to Table 2 and 3 respectively. The absorbance reading were done in triplicates to validate data accuracy for the ANOVA analysis and presented on the 3-D surface plots. The response (Y) was calculated using the coefficients of quadratic equation:

$$Y = A + B + C + D + A^2 + B^2 + C^2 + D^2 + AB + BC + CD + AD \quad \text{..... (24)}$$

where A, B, C, and D are pH, concentration, dosage and temperature respectively[23].

2.7.1. Optimization

Table 2 Process Variables and Levels

Factors	Low (-1)	Mean (0)	High (+)
pH	1	7.5	14
Conc. (mgL-1)	50	150	250
Dosage (g)	0.1	1.05	2.0
Temperature (oC)	30	50	70

Process optimization was achieved using the numerical node of the design expert software. The three studied variables were targeted within the range (high and low) and the adsorption capacity (response) was targeted at the maximum. The program integrates individual factors at tuneable levels and output response. Variation of the factors produces an important result which leads to optimal conditions. The 3-D plots represent the effect of two factors simultaneously, showing the predicted values from the coded model for the combinations of the −1 and +1 level of the four factors under consideration.

3. Results and discussion

3.1. FTIR characterization of the AGP

Fourier transform infra red (FTIR) technique was used to detect the functional groups present in AGP and to identify the ones involved in the adsorption of safranin dye. The IR spectrum of AGP after the dye adsorption shown in Figure 1.The prominent band at 3050 cm^{-1} was assigned to sp^3 C – H of the cellulose in the adsorbent. The stretching vibration frequencies at 3420 and 3470 cm^{-1} were assigned to O – H group in the adsorbent. The bands at 1730 and 1720 cm^{-1} indicated ν (C = O) of the adsorbent. Meanwhile, the symmetric stretch at 1600 and 1620 cm^{-1} were assigned to C = C groups of the aromatic compounds, suggesting the functional groups interaction between the adsorbent and dye molecules. The band at 1100 cm^{-1} was assigned to the C–O group. The changes in FTIR spectrum confirmed the effect of modification of the groundnut pods with mostly bonded ν(O-H) which explained the inter and intra-molecular hydrogen bonding of the polymeric compounds (macromolecular association). This is in agreement with O-H vibration frequency observed in cellulose and lignin, thus showing the presence of free hydroxyl groups on the modified adsorbent [24]. The prominent shift was due to the effect of activation in the adsorbent (AGP) indicating its usefulness in the adsorption processes.

3.2. SEM analysis

The SEM images of raw groundnut pods and activated groundnut pods (AGP) are shown in Fig 2. It was deduced that the AGP became compact after adsorption of safranin dye. Several large pores in a rod shape were shown on the surface of the activated groundnut pods (AGP) as compared with raw groundnut powder. The open pores on AGP corroborated the effective activation process on the surface of the adsorbent which enhances adsorption of dye [25]. The EDX analysis shown a high percentage of carbon in the AGP which make it suitable and promising adsorbent.

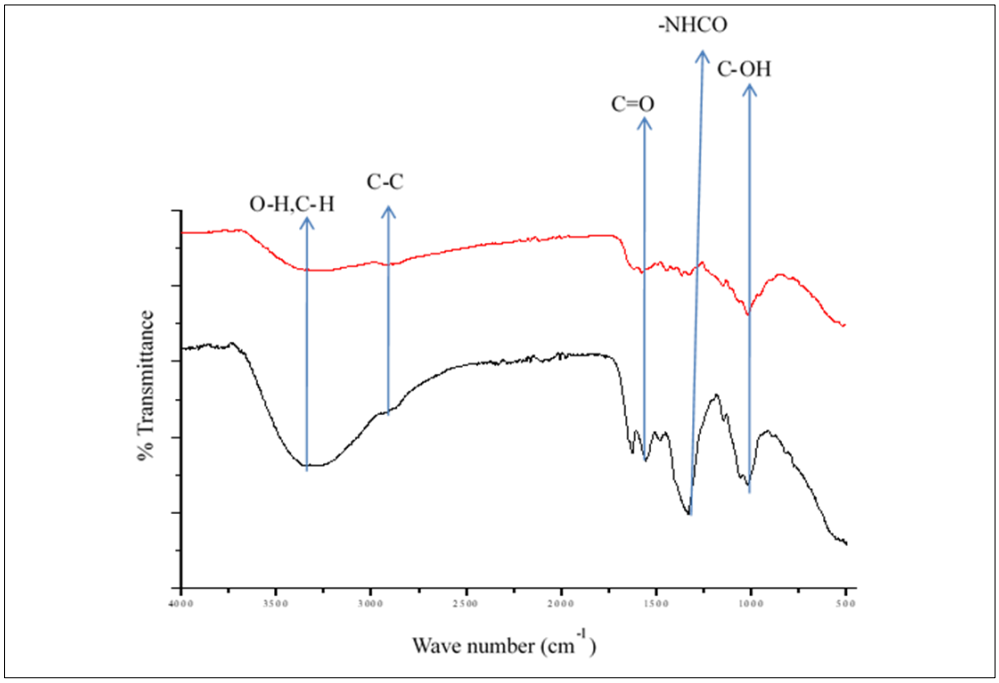

Figure 2 FTIR of AGP before and after adsorbed with safranin dye

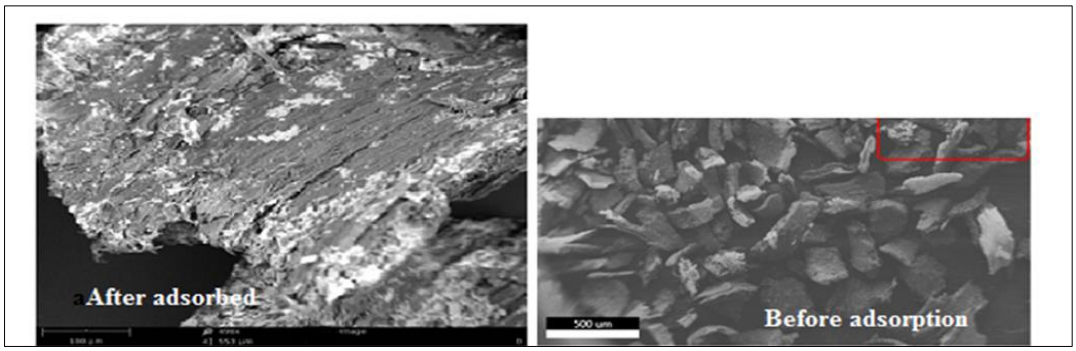

Figure 3 SEM analysis of AGP before and after the adsorption of safranin dye

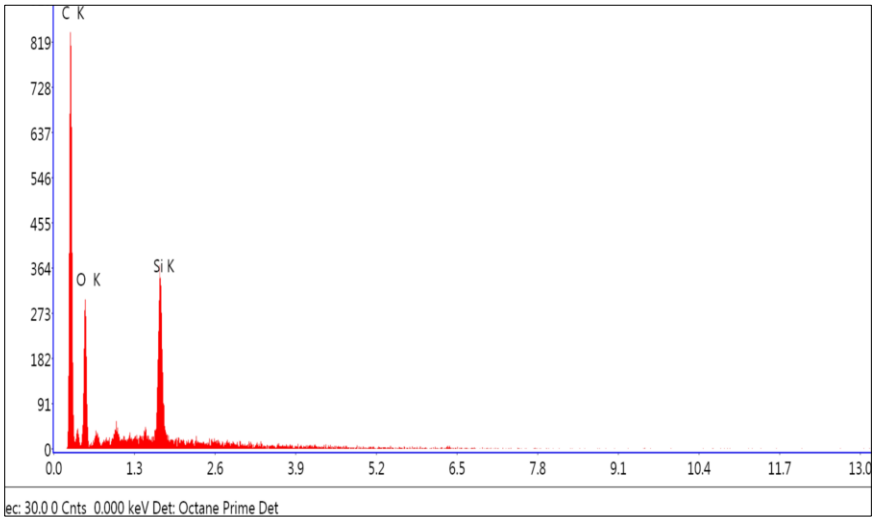

Figure 4 EDAX of AGP Adsorption of safranin dye

3.3. Adsorbent Dosage Study

The adsorbent dosage increase at 0.1 - 1.5g proportionally increases its removal efficiency ranging from 92.5 - 98.6 % as presented in Figure 5, which could be attributed to the increase in adsorption sites of the AGP. [26]. The reduction of the removal efficiency noted on further increase in the adsorbent dosage resulted from particle interactions that collapsed the active sites of the adsorbent [27].

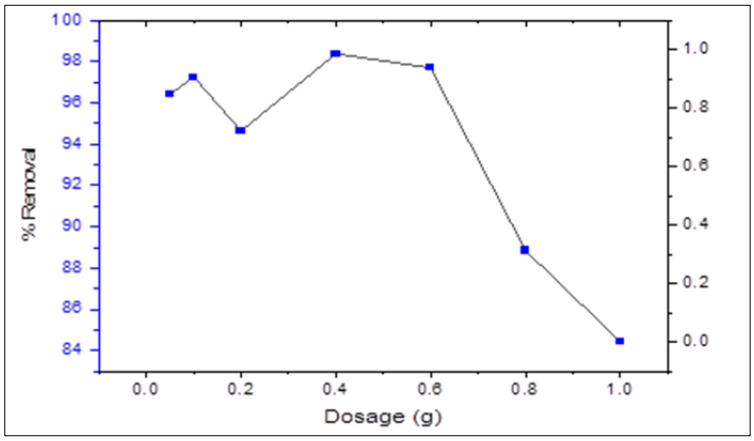

Figure 5 Adsorbent dosage against % removal of safranin dye

3.4. Solution pH study of the adsorption of safranin dye

The removal efficiency of the dye increases with the pH of the media increase as presented in Figure 6. pH affects the chemical properties of the dye solution, the adsorbent surface charge, as well as interactions in the media [28].The maximum 95% removal efficiency was obtained for the dye solution at pH 10.The acidic pH lowers the adsorption of the adsorbate because of its competition with the hydrogen ion on the available adsorption sites [29].

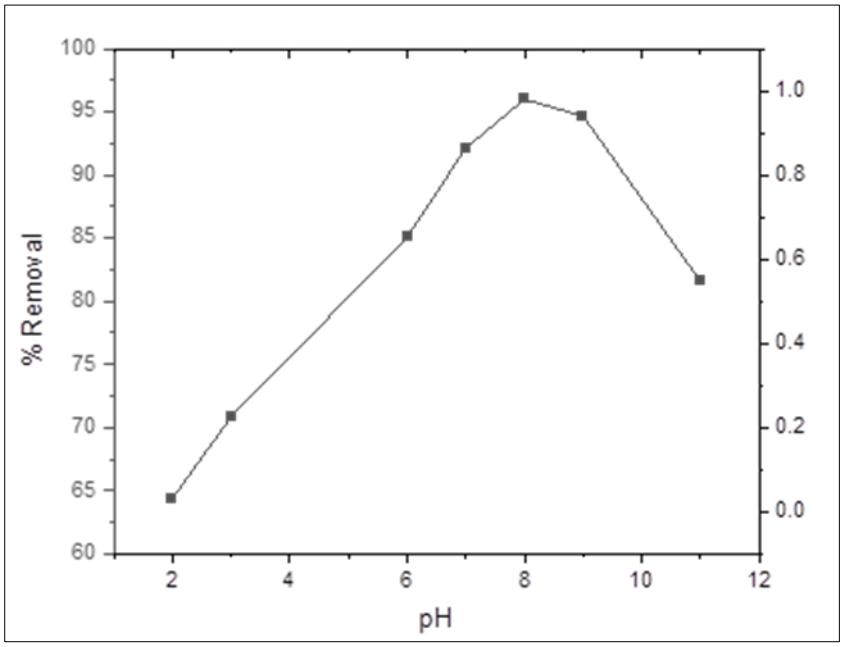

Figure 6 The Plot of solution pH against % Removal of safranin dye

3.5. Effect of initial concentration and contact time of safranin dye

Removal of dye from aqueous solution depends on the initial dye concentration and contact time. The quantity of dye removed increases proportionally as initial concentration increases also is adsorption. Safranin dye was rapidly removed in the first 15 minutes, maintained for the next 30 minutes then continued steadily until equilibrium. Adsorption capacities at equilibrium increases from 5.45 to 16.89 mg/g as the initial concentrations increases from 50 to 250 ppm.

3.5.1. Energy dispersive X-ray spectroscopy (EDX) of the AGP

Elemental analyses of raw groundnut pods and AGP samples are presented in Figure 4, Tables 3 and 4 respectively. The results showed significant carbon content increased from 64.93 to 89.86% in AGP. The most effective adsorbent contained the highest amount of carbon. Thus, the higher the amount of carbon in the sample, the more effective the adsorbent in removing the adsorbate.

Table 3 EDX elemental analysis of raw groundnut pods

Elements	Wt %	At %	K-ratio	Z	A	F
Carbon	64.93	72.67	0.4221	1.0113	0.6900	1.0000
Oxygen	29.43	25.35	0.3106	0.9374	0.5836	1.0002
Silicon	3.63	1.37	0.0341	0.9618	0.4351	1.0000
Potassium	2.00	0.61	0.0216	0.9176	0.9411	1.0000
Total	100.0	100.0				

Wt % = weight %, At % = Atomic %, K-ratio = Intensity ratio, ZAF = correction factors

Table 4 EDX elemental analysis of AGP

Elements	Wt %	At %	K-ratio	Z	A	F
Carbon	89.86	84.42	0.6749	1.0564	0.8649	1.0000
Oxygen	16.75	14.38	0.0840	0.9917	0.5058	1.0000
Zinc	2.92	0.72	0.0167	0.7196	0.7955	0.9982
Tantalum	6.47	0.49	0.0380	0.5027	1.1362	1.0281
Total	100.0	100.0				

Wt % = weight %, At % = Atomic %, K-ratio = Intensity ratio, ZAF = correction factors.

3.6. Adsorption Kinetics

The meaning of adsorption kinetics is a function of elaborate analysis of time dependent adsorption data. The process was characterized by mechanisms such as; chemical interactions between the adsorbent (AGP) and adsorbate (safranin dye), mass transfer of the adsorbate into and within the adsorbent or combination of these mechanisms, hence combination of models were required to elucidate the mechanism of adsorption. The pseudo first-order, pseudo second-order as well as Elovich kinetic models were used to examine the kinetics of adsorption data which are depicted Fig 7, 8 and 9 while the parameters for these fits are presented in Tables 5, 6 and 7 respectively.

By considering the values of the regression coefficients R^2 for the models, error function analyses and the closeness of the Q_e determined experimentally with the theoretical values showed that pseudo- second order kinetic model was much favoured, suggesting physical interactions between the adsorbent and adsorbate [30]. The Elovich kinetic model fit (Figure 9) agreed with the experimental data (Table 7) and showed that $R^2 > 0.90$, the values β_{el} indicate the available site for adsorption decreases with increase dye concentrations. The positive values of these constants confirmed the model, hence Elovich model properly explained the initial kinetics of adsorption of the dye onto the adsorbent as previously reported in literature [31].

Table 5 Pseudo first order Kinetic data of Safranin dye adsorption

Conc. (mgL^{-1})	50	100	150	200	250
$Q_{e(\ Exp)}$ (mgg^{-1})	1.517	2.695	4.746	3.705	4.230
$Q_{e(cal)}$ (mgg^{-1})	2.193	4.463	5.825	5.540	5.620
$k_1(min^{-1})$	0.022	0.011	0.008	0.012	0.200
R^2	0.999	0.998	0.998	0.998	0.997
% SSE	3.288	4.310	5.175	3.147	1.811
RMSE	0.047	0.096	0.135	0.104	0.081
HYBRID	1.588	2.575	2.843	2.215	1.632

Table 6 Pseudo Second Order Kinetic data of safranin dye adsorption

Conc. (mgL-1)	50	100	150	200	250
Qe(cal) (mgg-1)	1.614	2.694	4.275	4.322	4.319
k2 (gmg-1min-1)	0.046	0.047	0.045	0.058	0.062
R2	0.999	0.999	0.999	0.999	0.998
% SSE	0.000	0.000	0.004	0.001	0.038
RMSE	0.000	0.000	0.004	0.002	0.013
HYBRID	0.022	0.003	0.076	0.045	0.222

Table 7 Elovich kinetic data of safranin dye adsorption

Conc. (mgL^{-1})	**50**	**100**	**150**	**200**	**250**
$Qe_{(cal)}$ (mgg^{-1})	2.467	4.778	7.138	9.530	11.821
α_{el} ($gmg^{-1}\ min^{-1}$)	6.300	37.103	8.613	13.415	15.309
β_{el} (mgg^{-1})	3.157	1.892	0.968	0.744	0.521
R^2	0.994	0.995	0.996	0.997	0.999
% SSE x 10^7	3.791	2.614	2.343	0.254	0.581
RMSE x 10^4	1.905	3.057	4.296	0.189	0.357
HYBRID	0.005	0.003	0.004	0.021	0.014

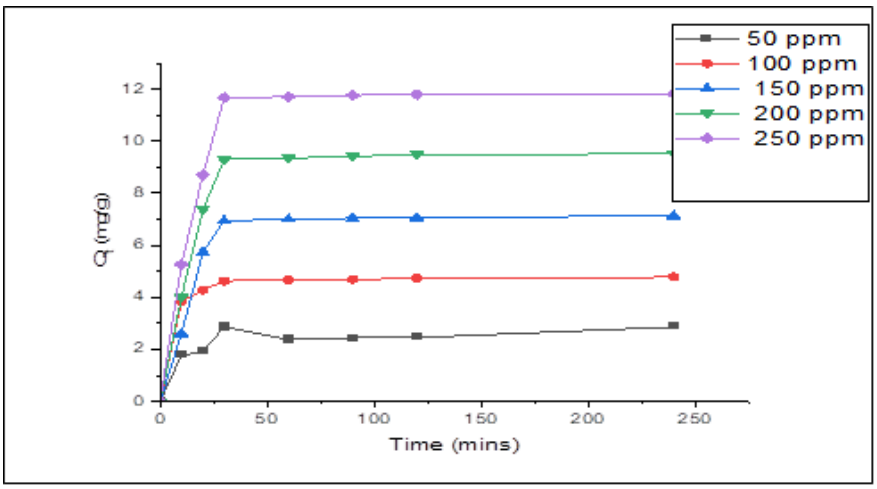

Figure 7 Pseudo-first Order Kinetic Plot of Q_t (mgg^{-1}) against Time (min)

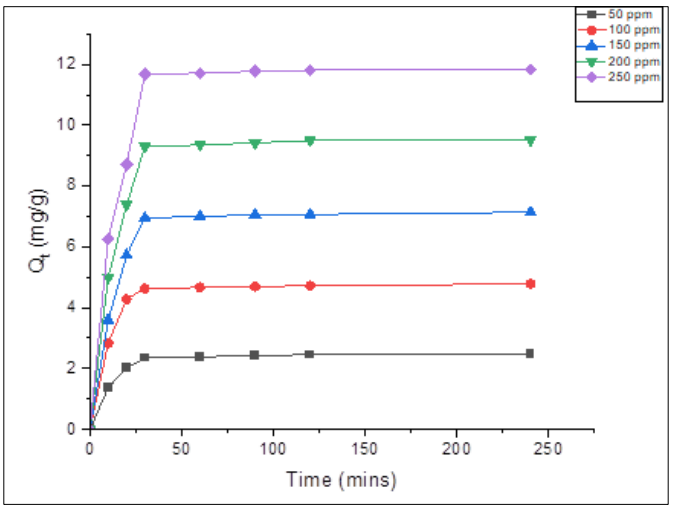

Figure 8 Pseudo-Second order kinetic plot of Q_t (mgg^{-1}) against Time (min)

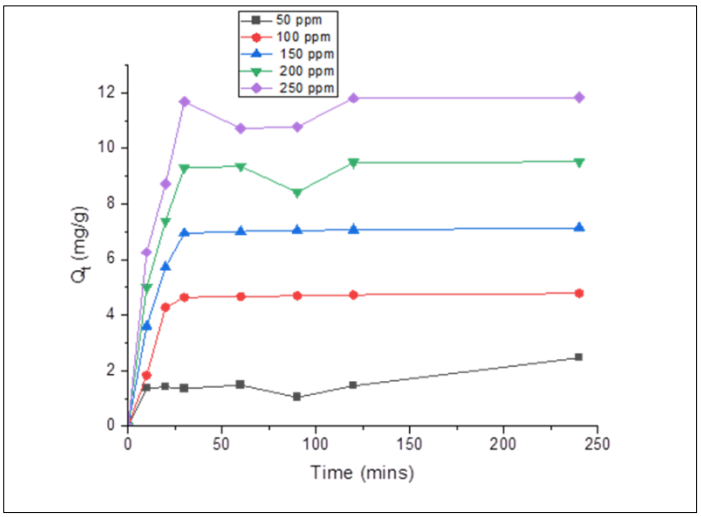

Figure 9 Elovich kinetic plot of Q_t (mgg^{-1}) against Time (min)

3.7. Adsorption isotherm

Adsorption isotherms described the phenomenon governing the release or mobility of a substance from the aqueous media to a solid-phase at a constant temperature and pH. Interpretations of these information are critical to the overall improvement of adsorption mechanism pathways and effective design of adsorption system [32]. The adsorption isotherm models used to confirm the adsorption of safranin dye onto AGP are presented in Figure 10 and parameters (Table 8). The isotherm parameters revealed that the entire isotherms model investigated fit very well with the data and correlation coefficient R^2 values in the order of Langmuir > Freundlich > Tempkin>Dubinin-Radushkevich. This suggested a monolayer adsorption of safranin onto the adsorbent with maximum adsorption capacities (Q_{max}) of 45.45 mgg^{-1}. The K_L values <1 indicated a favourable adsorption. Freundlich parameters confirmed the heterogeneity nature of the surface of adsorbent, the $^1/n$ value of < 1 indicates a normal Langmuir isotherm, otherwise cooperative adsorption [33]. The Tempkin isotherm parameters and the R^2 values showed favourable fits for the dyes, to imply that adsorption process is characterized by uniform distribution of binding energies. The mean free energies obtained for the adsorption of the dye is< 8 kJ/mol, confirming the physisorption adsorption as suggested by the kinetic fit[34].

Table 8 Adsorption isotherms parameters for Safranin dye

Isotherms	Parameters	Values
Langmuir	Q_{max} (mgg^{-1})	45.45
	L ($L\ mg^{-1}$)	0.255
	K_L	0.097
	R^2	0.998
Freudlich Isotherm	K_F ($g\ mg^{-1}\ min^{-1/n}$)	5.460
	$^1/n$	0.351
	R^2	0.997
Tempkin Isotherm	b_T	736.684
	a_T ($L\ mg^{-1}$)	4.544
	R^2	0.995
R-D Isotherms	Q_S (mgg^{-1})	15.329
	β x 10^6 $(mol\ J^{-1})^2$	1.20E+00
	E($kJ\ mol^{-1}$)	0.646
	R^2	0.990

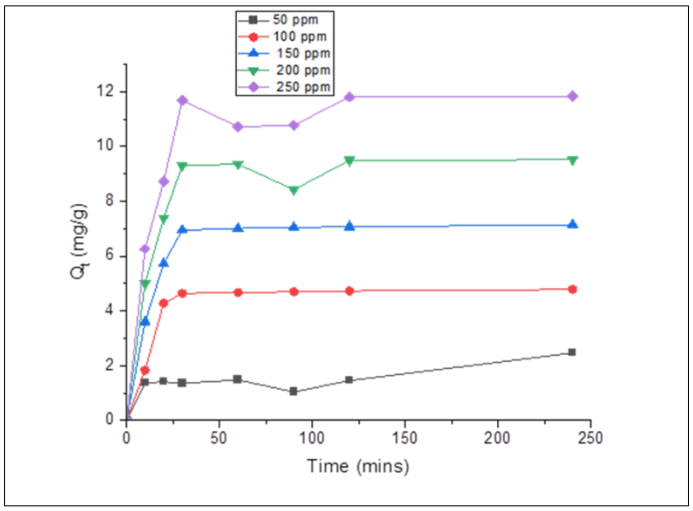

Figure 10 Isotherm plots of Q_e (mgg^{-1}) against C_e (mgL^{-1})

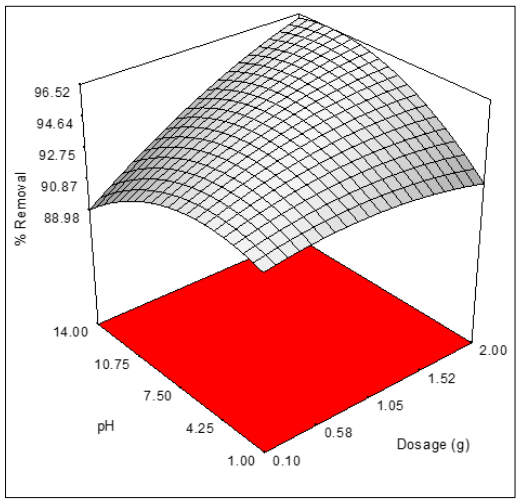

(a)

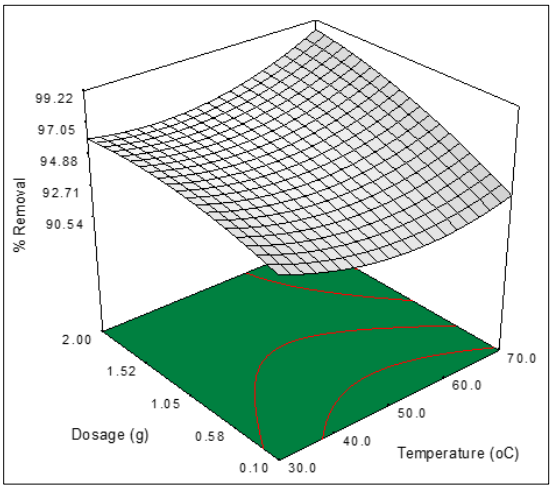

(b)

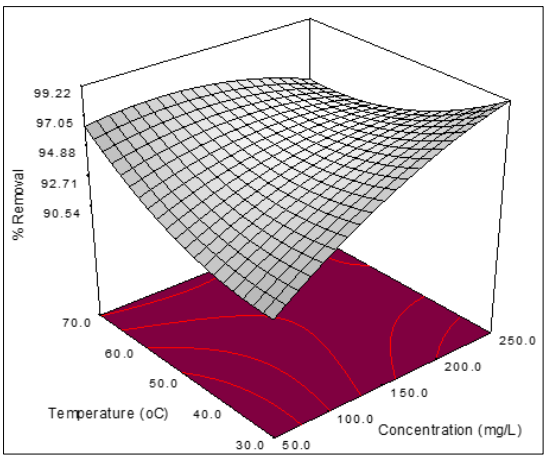

(c)

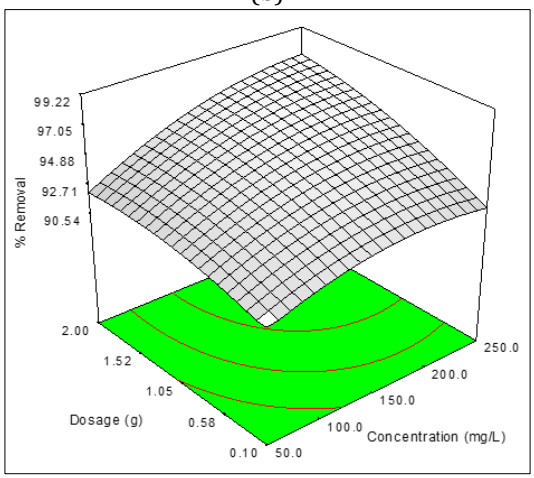

(d)

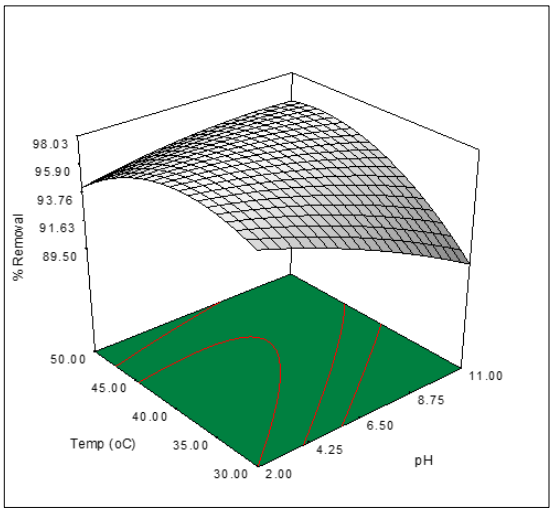

(e)

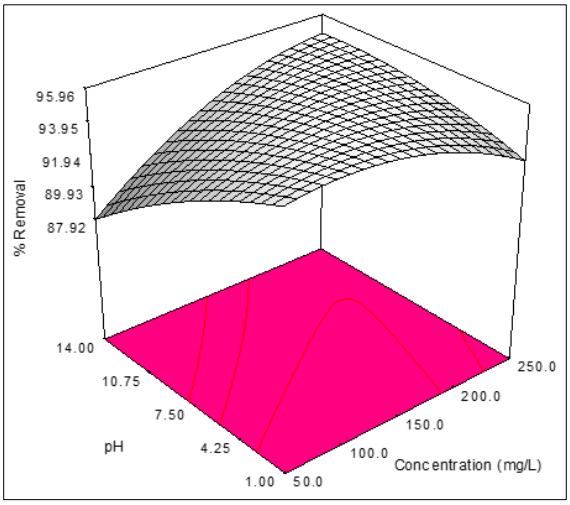

(f)

Figure 11 Response surface plots for the removal efficiency of safranin dye

Table 9 Box – Behnken matrix for safranin-o dye adsorption

Conc. (mg/L)	Temp (°C)	Dosage (g)	pH	% Removal		
				Actual Value	Predicted Value	Residue
150	70	1.05	1	98.55	98.43	0.12
150	70	2	7.5	97.67	96.99	0.68
50	30	1.05	7.5	92.76	93	-0.24
250	50	0.1	7.5	91.82	91.87	-0.05
150	70	1.05	14	85.9	86.87	-0.97
250	50	2	7.5	90	90.31	-0.31
50	50	1.05	14	85.87	85.44	0.43
250	70	1.05	7.5	95.43	96.44	-1.01
50	70	1.05	7.5	98.75	98.23	0.52
150	50	1.05	7.5	95.26	95.12	0.14
150	50	2	14	97.43	97.87	-0.44
150	50	1.05	7.5	85.12	85.02	0.1
150	30	0.1	7.5	82.98	82.45	0.53
50	50	0.1	7.5	88.54	88.39	0.15
250	30	1.05	7.5	99.04	98.89	0.15
250	50	1.05	1	91.45	91.32	0.13
150	50	0.1	1	93.21	93.15	0.06
50	50	2	7.5	91.82	92.17	-0.35
150	30	1.05	1	99.35	99.15	0.2
150	30	2	7.5	94.21	94.1	0.11

150	50	1.05	7.5	98.56	98.43	0.13
50	50	1.05	1	92.82	93.11	-0.29
150	50	0.1	14	81.97	81.93	0.04
150	50	1.05	7.5	85.97	86.32	-0.35
150	50	2	1	92.35	91.43	0.92
250	50	1.05	14	94.34	93.87	0.47
150	30	1.05	14	96.98	96.25	0.73

Table 10 Regression Statistics for Safranin-o dye Adsorption Process

Source	**Std. dev.**	**R^2**	**Adj. R^2**	**Pre. R^2**	**Comment**
Linear	6.09	0.8150	0.8631	0.7712	
2FI	3.35	0.8635	0.8951	0.5324	
Quadratic	**0.75**	**0.9770**	**0.9500**	**0.978**	**Suggested**
Cubic	0.035	1.0000	1.0000	0.9135	**Aliased**

Where FI= Factoral interaction, R^2= Correlation coefficient, Std. dev = Standard deviation, Adj = Adjusted, Pre = Predicted

The significance of the model including the terms in the equation were determined from the Analysis of variance (ANOVA), regression and model summary statistics using parameters such as the F-test, P-value and the sum of squares and the results presented. The higher F-values obtained for the safranin dye show that the models are significance with p-values of <0.0001 indicating that the contribution of the obtained values is insignificant. For the removal of the Safranin dye, adsorbent dosage and temperature were found to be more significant among all the parameters, given their highest sum of a square and F-test values respectively[35]. However, the combined effect of pH and adsorbent dosage on removal efficiency was predominant among all the possible combinations for the dye, whereas dye concentration was the most dominants of the squared term[36]. The non-significant obtained from the lack of fit value implied the perfect fit of experimental data in the chosen quadratic model. The correlation coefficients were estimated for the accuracy of experimental results and shown that, the predicted R^2 and adjusted R^2 were in reasonable agreement with each other which implied that the variation about the mean and capability of the model to predict the response was in the acceptable range. Adequate precision measured the signal to noise ratio and the desirable ratio was 4, the ratio 18.45 obtained for the Safranin dye removal indicated an adequate signal. The models obtained therefore can be used to navigate the design space.

The maximum removal efficiency of 94.73% was observed within the pH 2 - 12 at 40^{o}C, lowering temperature below the range minimized the removal efficiency (Figure 11a - f). The combined effect of pH and adsorbent dosage showed that the simultaneous increase of both factors led to an increase in removal efficiency from 88.9 to 97.2 %. The effects pH and initial dye concentration as shown in Figure 11f indicated that pH increase with dye concentration raised the efficiency by 10%. Removal efficiency decreased from 94.73 to 84.31 % as the adsorbent dosage decreased with temperature initially at 40^{o}C. The combined effect of concentration and temperature showed an initial decrease in efficiency as the concentration increased between 50 and 250 mg/L, further increase in concentration with temperature raised the efficiency to 89.6% from86.5%. Simultaneous increases in the initial dye concentration with adsorbent dosage increase the removal efficiency from 85.6 to 96.8%. These results of the statistical analysis data confirmed the experimental data to a significant degree of certainty. It could be concluded that experimental procedure followed the predicted optimized condition by selected quadratic model.

Table 11 ANOVA analysis of Box-Behnken model for Safranin dye adsorption

Source	Sum of Squares	DF	Mean Square	F Value	Prob > F	
Model	824.6735	14	58.90525	6.498284	0.0004	significant
pH	517.196	1	517.196	57.0558	< 0.0001	
Concentration	17.56896	1	17.56896	1.938165	0.1856	
Dosage	0.084706	1	0.084706	0.009345	0.9244	
Temperature	116.7036	1	116.7036	12.87446	0.0030	
pH^2	23.95978	1	23.95978	2.643184	0.1263	
$Concentration^2$	1.626577	1	1.626577	0.17944	0.6783	
$Dosage^2$	0.222839	1	0.222839	0.024583	0.8776	
$Temperature^2$	50.97903	1	50.97903	5.623882	0.0326	
pH x Conc.	0.015203	1	0.015203	0.001677	0.9679	
pH x Dosage	8.093741	1	8.093741	0.892882	0.3607	
pH x Temp.	21.78136	1	21.78136	2.402866	0.1434	
Conc.xDosage	5.134983	1	5.134983	0.566479	0.4641	
Conc. x Temp.	67.50594	1	67.50594	7.447091	0.0163	
DosagexTemp	0.416799	1	0.416799	0.04598	0.8333	
Residual	126.9063	14	9.064739			
Lack of Fit	1103.1836	10	10.31836	1.739821	0.3123	not significant
Pure Error	0.32279	4	0.32279			
Cor Total	651.5798	28				

4. Adsorption Thermodynamic Study

The van't Hoff plot (Fig.12) for the adsorption of safranin dye using AGP and the thermodynamic parameters (Tab.12) showing enthalpy change (ΔH) and entropy change (ΔS) had positive values of 66.43 $KJmol^{-1}$ and 145.375 $Jmol^{-1}K$ respectively, hence, endothermic adsorption process and this suggest that some amount of heat was consumed to transfer dye ions from aqueous solution to the active site of AGP. The positive value of ΔS indicates an increase in the degree of randomness of the system with changes in the hydration of the adsorbed dye ions [37].The negative values of Gibb's energy indicated the spontaneity of the adsorption process and the decrease of the values with increasing temperature indicated more efficient adsorption at higher temperatures.

4.1. Thermodynamic Analysis

The thermodynamic parameters, ΔG^o, ΔH^o and ΔS^o explain the feasibility, spontaneity and the nature of adsorbate-adsorbent interactions during the adsorption process[38].The equilibrium constant in term of the adsorbate (C_e), adsorbent dosage (m) and adsorbed quantity (Q_e) could be written as:

$$K = \frac{Q_e}{C_e * m} \quad \text{..... (25)}$$

Where k is the equilibrium adsorption constant[39]

$$\Delta G = \Delta H - T\Delta S \quad \text{..... (26)}$$

T is the temperature in Kelvin, other parameters had already been discussed.

$$\Delta G = -RT \ln K \quad \text{..... (27)}$$

R is the gas constant and equal to 8.314 kJmol^{-1}

$$\ln k = \frac{\Delta S}{R} - \frac{\Delta H}{RT} \quad \text{..... (28)}$$

The van't Hoff plot, (In K_D versus 1/T) for the adsorption process gives the slope and intercept from which thermodynamic parameters were obtained.

$$C = \frac{\Delta S}{R} \quad \text{..... (29)}$$

$$m = \frac{\Delta H}{R} \quad \text{..... (30)}$$

Table 12 Thermodynamic Parameters for the adsorption of safranin dye

Temp (K)	lnKd	ΔG (kJ mol-1)	ΔH (kJ mol-1)	ΔS (J mol-1 K-1)	R2
308.15	1.282	-3.431	66.43	145.375	0.941
313.15	1.705	-4.317			
318.15	1.785	-5.204			
323.15	2.404	-6.091			

In k = equilibrium constant, ΔG = Change in Gibb's free energy, ΔH = Enthalpy change; ΔS = Entropy change, R^2 = Correlation coefficient.

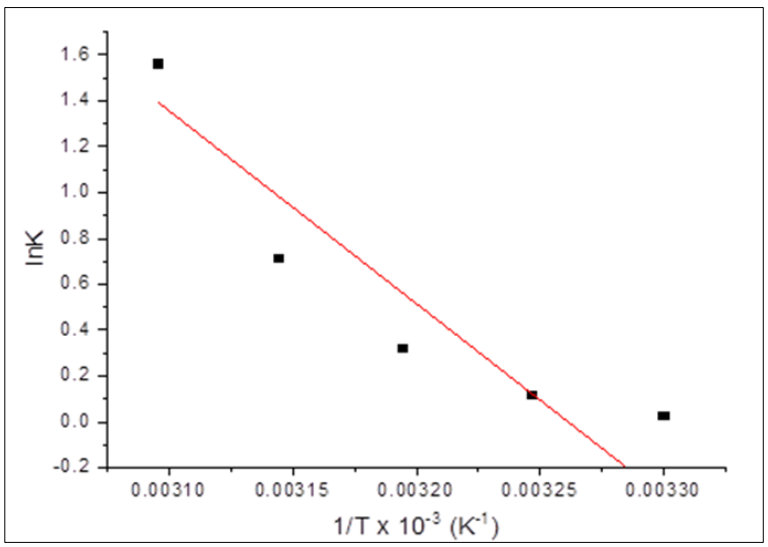

Figure 12 Van't Hoff plot of lnK against 1/T

Table 13 Physicochemical Parameters of the AGP

Raw Groundnut pods Composition (%)	Proximate
Crude Protein	13.28 ± 1
Ether Extract	15.67 ± 1
Crude Fat	1.89 ± 1
Ash content	35.89 ± 1
Cellulose content	65.43 ± 1
Moisture content	5.50 ± 1
Dry Matter	94.50 ± 1
NFE	55.09 ± 1

5. Conclusion

Activated carbon derived from groundnut pods biomass was prepared and applied to remove safranin dye from aqueous solution. The treatment adopted batch adsorption method considering some parameters like contact time, initial dye concentration, solution pH, adsorbent dosage and temperature dependent. The kinetics of adsorption of the dye was best explained with pseudo second-order kinetic while Langmuir isotherm model fitted the equilibrium data with monolayer adsorption capacity of 45.45 mg/g. The statistical analysis showed that the predicted models are suitable for the prediction of the adsorption process with $R^2 > 0.9$. The thermodynamic parameters proved that the adsorption process was feasible, spontaneous, endothermic and random in nature.

Compliance with ethical standards

Acknowledgments

The Authors appreciate Research Innovate Strategy and Administration (RISA) of Caleb University for financing the publication of this article.

Disclosure of conflict of interest

Authors declared no conflict of interest.

References

[1] El Qada E.N., S. J. Allen, and G. M. Walker, "Adsorption of basic dyes from aqueous solution onto activated carbons," Chem. Eng. J., vol. 135, no. 3, pp. 174–184, 2008.

[2] Giraldo L. and J. C. Moreno-Pirajan, "Synthesis of activated carbon mesoporous from coffee waste and its application in adsorption zinc and mercury ions from aqueous solution," E-Journal Chem., vol. 9, no. 2, pp. 938–948, 2012.

[3] Park H. and W. Choi, "Visible light and Fe (III) -mediated degradation of Acid Orange 7 in the absence of H2O2," J. Photochem. Photobiol. A Chem., vol. 159, pp. 241–247, 2003.

[4] Muthuraman G., T. T. Teng, C. P. Leh, and I. Norli, "Extraction and recovery of methylene blue from industrial wastewater using benzoic acid as an extractant," J. Hazard. Mater., vol. 163, pp. 363–369, 2009.

[5] Vadivelan V. and K. Vasanth Kumar, "Equilibrium, kinetics, mechanism, and process design for the sorption of methylene blue onto rice husk," J. Colloid Interface Sci., vol. 286, no. 1, pp. 90–100, 2005.

[6] Garcıa M., I. Garmendia, and J. Garcıa, "Influence of Natural Fiber Type in Eco-Composites," J. Appl. Polym. Sci., vol. 107, pp. 2994–3004, 2008.

[7] Wang W., M. Sain, and P. A. Cooper, "Study of moisture absorption in natural fiber plastic composites," Compos. Sci. Technol., vol. 66, pp. 379–386, 2006.

[8] Fungaro D.A., M. Bruno, and L. C. Grosche, "Adsorption and kinetic studies of methylene blue on zeolite synthesized from fly ash," Desalin. Water Treat., vol. 2, no. 1–3, pp. 231–239, 2009.

[9] Adeogun A.I., J. A. Akande, M. A. Idowu, and S. O. Kareem, "Magnetic tuned sorghum husk biosorbent for effective removal of cationic dyes from aqueous solution: isotherm, kinetics, thermodynamics and optimization studies," Appl. Water Sci., vol. 9, no. 7, pp. 1–17, 2019.

[10] Porter J.F., G. McKay, and K. H. Choy, "The prediction of sorption from a binary mixture of acidic dyes using single- and mixed-isotherm variants of the ideal adsorbed solute theory," Chem. Eng. Sci., vol. 54, no. 24, pp. 5863–5885, 1999.

[11] Kapoor A. and R. T. Yang, "Correlation of equilibrium adsorption data of condensible vapours on porous adsorbents," Gas Sep. Purif., vol. 3, no. 4, pp. 187–192, 1989.

[12] Aksu S.T.Z., U. Acıkel, E. Kabasakal, "Equilibrium modelling of individual and simultaneous biosorption of chromium (VI) and nickel (II) onto dried activated sludge," Water Res., vol. 36, pp. 3063–3073, 2002.

[13] Ho R., General Linear Model: Repeated Measures Analysis: In: Ho R. Handbook of Univariate and Multivariate Data Analysis and Interpretation with SPSS. 2006.

[14] Kumar A., B. Prasad, and I. M. Mishra, "Adsorptive removal of acrylonitrile by commercial grade activated carbon: Kinetics, equilibrium and thermodynamics," J. Hazard. Mater., vol. 152, no. 2, pp. 589–600, 2008.

[15] Akinhanmi F.T., A. I. Adeogun, and A. Adegbuyi, "Removal of Cu2+ from aqueous solution by adsorption onto quail eggshell: Kinetic and isothermal studies," J. Environ. Biotechnol. Res., vol. 5, no. 1, pp. 1–9, 2016.

[16] Wang S., L. Li, H. Wu, and Z. H. Zhu, "Unburned carbon as a low-cost adsorbent for treatment of methylene blue-containing wastewater," J. Colloid Interface Sci., vol. 292, pp. 336–343, 2005.

[17] Dakhil I.H., "Acomparative Study for Removal of Dyes from Textile Effluents by Low Cost Adsorbents To cite this article :," Mesopotamia Environ. J., vol. 9, pp. 1–9, 2016.

[18] Shahwan T., "Lagergren equation: Can maximum loading of sorption replace equilibrium loading?," Chem. Eng. Res. Des., vol. 95, pp. 172–176, 2015.

[19] Ho Y.S., J. C. Y. Ng, and G. McKay, "Kinetics of pollutant sorption by biosorbents: Review," Sep. Purif. Methods, vol. 29, no. 2, pp. 189–232, 2000.

[20] Elovich S. and OG Larionov, "Theory of adsorption from nonelectrolyte solutions on solid adsorbents.," Bull. Acad. Sci. USSR Chem. Sci., vol. 11, pp. 198–203, 1962.

[21] Halsey G.D., "On Multilayer Adsorption," J. Am. Soc., vol. 74, no. 4, pp. 1082–1083, 1952.

[22] Zhao M., Z. Tang, and P. Liu, "Removal of methylene blue from aqueous solution with silica nano-sheets derived from vermiculite," J. Hazard. Mater., vol. 158, no. 1, pp. 43–51, 2008.

[23] Ebrahimi A., E. Pajootan, M. Arami, and H. Bahrami, "Optimization, kinetics, equilibrium, and thermodynamic investigation of cationic dye adsorption on the fish bone," Desalin. Water Treat., vol. 53, no. 8, pp. 2249–2259, 2015.

[24] Khandanlou R., M. Bin Ahmad, K. Shameli, and K. Kalantari, "Synthesis and Characterization of Rice Straw/Fe3O4 Nanocomposites by a Quick Precipitation Method," Molecules, vol. 18, pp. 6597–6607, 2013.

[25] Asif Tahir M., H. N. Bhatti, and M. Iqbal, "Solar Red and Brittle Blue direct dyes adsorption onto Eucalyptus angophoroides bark: Equilibrium, kinetics and thermodynamic studies," J. Environ. Chem. Eng., vol. 4, no. 2, pp. 2431–2439, 2016.

[26] Hoseinzadeh E., M. R. Samarghandi, G. McKay, N. Rahimi, and J. Jafari, "Removal of acid dyes from aqueous solution using potato peel waste biomass: A kinetic and equilibrium study," Desalin. Water Treat., vol. 52, no. 25–27, pp. 4999–5006, 2014.

[27] Kakavandi B., A. Takdastan, N. Jaafarzadeh, M. Azizi, A. Mirzaei, and A. Azari, "Application of Fe3O4@C catalyzing heterogeneous UV-Fenton system for tetracycline removal with a focus on optimization by a response surface method," J. Photochem. Photobiol. A Chem., vol. 314, pp. 178–188, 2016.

[28] Ahsaine H.A., M. Zbair, Z. Anfar, Y. Naciri, El haouti R, N. El Alem, M. Ezahri, "Cationic dyes adsorption onto high surface area ' almond shell ' activated carbon : Kinetics , equilibrium isotherms and surface statistical modeling," Mater. Today Chem., vol. 8, pp. 121–132, 2018.

[29] Bestani B., N. Benderdouche, B. Benstaali, M. Belhakem, and A. Addou, "Bioresource Technology Methylene blue and iodine adsorption onto an activated desert plant," Bioresour. Technol., vol. 99, pp. 8441–8444, 2008.

[30] Akpomie K.G., O. M. Fayomi, C. C. Ezeofor, R. Sha'Ato, and W. E. Van Zyl, "Insights into the use of metal complexes of thiourea derivatives as highly efficient adsorbents for ciprofloxacin from contaminated water," Trans. R. Soc. South Africa, vol. 74, no. 2, pp. 180–188, 2019.

[31] Vassileva P., A. Detcheva, I. Uzunov, and S. Uzunova, "Removal of Metal Ions from Aqueous Solutions Using Pyrolyzed Rice Husks: Adsorption Kinetics and Equilibria," Chem. Eng. Commun., vol. 200, no. 12, pp. 1578–1599, 2013.

[32] Ayawei N., A. N. Ebelegi, and D. Wankasi, "Modelling and Interpretation of Adsorption Isotherms," J. Chem., vol. 2017, 2017.

[33] Pathania D., S. Sharma, and P. Singh, "Removal of methylene blue by adsorption onto activated carbon developed from Ficus carica bast," Arab. J. Chem., vol. 10, pp. S1445–S1451, 2017.

[34] Ozdes D., C. Duran, H. B. Senturk, H. Avan, and B. Bicer, "Kinetics, thermodynamics, and equilibrium evaluation of adsorptive removal of methylene blue onto natural illitic clay mineral," Desalin. Water Treat., vol. 52, no. 1–3, pp. 208–218, 2014.

[35] Dhawane S.H., T. Kumar, and G. Halder, "Biodiesel synthesis from Hevea brasiliensis oil employing carbon supported heterogeneous catalyst: Optimization by Taguchi method," Renew. Energy, vol. 89, pp. 506–514, 2016.

[36] Inam E.I., U. J. Etim, E. G. Akpabio, and S. A. Umoren, "Simultaneous adsorption of lead (II) and 3,7-Bis(dimethylamino)-phenothiazin-5-ium chloride from aqueous solution by activated carbon prepared from plantain peels," Desalin. Water Treat., vol. 57, no. 14, pp. 6540–6553, 2016.

[37] Mall I.D., V. C. Srivastava, N. K. Agarwal, and I. M. Mishra, "Adsorptive removal of malachite green dye from aqueous solution by bagasse fly ash and activated carbon-kinetic study and equilibrium isotherm analyses," Colloids Surfaces A Physicochem. Eng. Asp., vol. 264, no. 1–3, pp. 17–28, 2005.

[38] Mohammadi N., H. Khani, V. K. Gupta, E. Amereh, and S. Agarwal, "Adsorption process of methyl orange dye onto mesoporous carbon material-kinetic and thermodynamic studies," J. Colloid Interface Sci., vol. 362, no. 2, pp. 457–462, 2011.

[39] Greluk M. and Z. Hubicki, "Kinetics, isotherm and thermodynamic studies of Reactive Black 5 removal by acid acrylic resins," Chem. Eng. J., vol. 162, no. 3, pp. 919–926, 2010.